JACS
JOURNAL OF THE AMERICAN CHEMICAL SOCIETY
Article
pubs.acs.org/JACS

Synthesis and Characterization of Iron–Nitrogen-Doped Graphene/Core–Shell Catalysts: Efficient Oxidative Dehydrogenation of *N*-Heterocycles

Xinjiang Cui,[†] Yuehui Li,[†] Stephan Bachmann,[‡] Michelangelo Scalone,[‡] Annette-Enrica Surkus,[†] Kathrin Junge,[†] Christoph Topf,[†] and Matthias Beller*[,†]

[†]Leibniz-Institut für Katalyse e.V., an der Universit Röstock, Albert Einstein Strasse 29a, 18059 Rostock, Germany
[‡]Process Research and Development, F. Hoffmann-La Roche Ltd., Grenzacherstrasse 124, 4070 Basel, Switzerland

Supporting Information

ABSTRACT: An important goal for nanocatalysis is the development of flexible and efficient methods for preparing active and stable core–shell catalysts. In this respect, we present the synthesis and characterization of iron oxides surrounded by nitrogen-doped-graphene shells immobilized on carbon support (labeled FeO_x@NGr–C). Active catalytic materials are obtained in a simple, scalable and two-step method via pyrolysis of iron acetate and phenanthroline and subsequent selective leaching. The optimized FeO_x@NGr–C catalyst showed high activity in oxidative dehydrogenations of several *N*-heterocycles. The utility of this benign methodology is demonstrated by the synthesis of pharmaceutically relevant quinolines. In addition, mechanistic studies prove that the reaction progresses via superoxide radical anions ($\cdot O_2^-$).

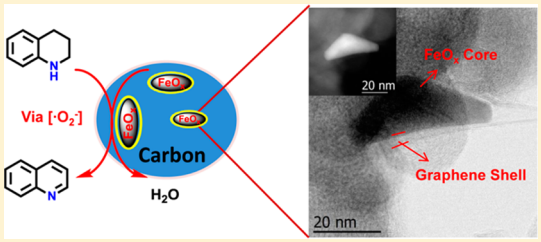

INTRODUCTION

Since the past decade, there exists an increasing interest in the development of iron-based organometallic catalysts for organic synthesis.[1] The inherent advantages of these complexes such as ready availability, low toxicity, and environmental friendliness make them preferred candidates for catalysis.[2] However, it should be noted that research on iron compounds has a long tradition; in fact, this is one of the oldest fields in chemistry and iron is also used widely and successfully in heterogeneous catalysis since the beginning of the last century.[3] In recent years, especially iron-based nanoparticles came into the focus of researchers because they feature novel properties different from the corresponding bulk materials.[4] Unfortunately, most of today's known highly active nano-iron catalysts are unstable and they are easily deactivated because of aggregation or leaching of the active metal in the reaction mixture. The development of core–shell structured materials provides a possibility to solve these problems. In case of iron nanoparticles, the resulting materials are often protected by organic or inorganic shells,[5] usually prepared at low temperature,[6] which limits the preparation and application of potential nanocatalysts.

Recently, iron–nitrogen–carbon (Fe/N/C) catalysts prepared by thermolysis of iron-ligated amines immobilized on high surface area have been studied in electro-catalysis, photocatalysis and organic synthesis.[4c,7] For these catalysts, N-doped materials are demonstrated to produce defects in graphene stacking in carbon based catalysts, which result in the formation of the O_2 absorption active sites. Interestingly, the activity of such Fe/N/C materials can be tuned by the choice of nitrogen precursors, the iron species, the carbon support morphology and the pyrolysis temperature.[8] Meanwhile, the N-doped graphene like materials have the ability to reductively adsorb O_2 and have been employed in the catalytic reduction of nitroarenes and also for reductive aminations.[9] Very recently, N-doped carbon based catalysts are applied in the selective oxidation of alcohols and amines, too.[10] To the best of our knowledge, related oxidative deydrogenations have not been investigated yet.

The catalytic dehydrogenation of *N*-heterocycles constitutes a fundamental process in organic synthesis. In recent years, several homogeneous catalysts were successfully employed in the catalytic dehydrogenations of *N*-heterocycles such as Ir-Pincer, Fe-Pincer, Ru-hydride complexes and so on.[11] On the other hand, heterogeneous catalysts such as Pd-HAP and CuAl-HT have also been used for these reactions.[12] Stahl et al. reported a homogeneous Ru–Co catalyst for the oxidation of *N*-heterocycles and Pd catalyzed the aerobic oxidation of cyclohexenes to aromatic arenes.[13] Furthermore, some heterogeneous oxidative systems such as Pd_3Pb, Pt-NW, AuNPs/C, Ru/Al_2O_3, Ru/Co_3O_4 and Ru/TiO_2 have been developed for these reactions.[14] However, most of the latter catalytic systems are based on noble metals or require harsh conditions and showed only poor functional-group tolerance. Thus, the development of inexpensive, earth copious and less toxic iron catalysts with a general and efficient activity for the

Received: June 2, 2015
Published: July 31, 2015

DOI: 10.1021/jacs.5b05674
J. Am. Chem. Soc. 2015, 137, 10652–10658

dehydrogenation of *N*-heterocycles is still challenging and of actual interest.

Inspired by the properties of the N-doped graphene materials to activate O_2 and encouraged by our recent investigations on the use of iron-based catalysts and N-doped heterogeneous materials,[9,15] we started to explore the preparation of novel iron−graphene materials and their application in the catalytic dehydrogenation of *N*-heterocycles. Herein, we report the preparation of novel iron oxide nanoparticles surrounded by a nitrogen-doped graphene shell supported on carbon (FeO_x@NGr−C) and describe for the first time their high stability and activity in catalytic oxidations of *N*-heterocycles.

RESULTS AND DISCUSSION

Typically, this new type of FeO_x@NGr−C catalyst was prepared using iron acetate, as the iron precursor and 1,10-phenanthroline (**L1**) as the nitrogen-rich ligand and the graphene precursor. Figures 1 and 2 depict the general

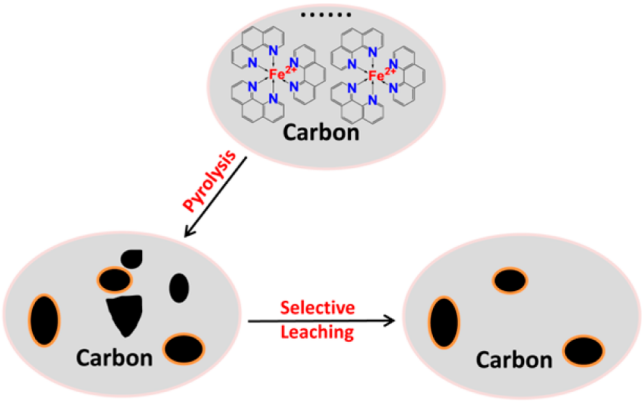

Figure 1. Schematic illustration showing the general procedure for the synthesis of FeO_x@NGr−C.

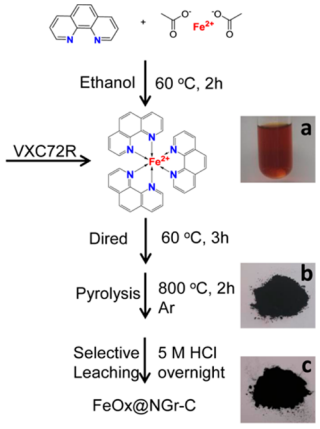

Figure 2. Schematic illustration for the preparation of the FeO_x@NGr−C. (a) Photograph of the Fe−phen complex. (b) Photograph of the catalyst precursor before pyrolysis. (c) Photograph of the obtained FeO_x@NGr−C.

preparation of the FeO_x@NGr−C catalyst. With the use of ethanol as the solvent, the formation of the iron complex and its uniform adsorption on the carbon support are facilitated. We suppose that the structure of the resulting immobilized metal-coordination polymer prevents the iron sites from agglomeration during the high temperature treatment and is favorable for the formation of well dispersed highly active sites. Moreover, the scaffold of 1,10-phenanthroline is relatively thermally stable, promoting the formation of graphene-like materials during pyrolysis (>600 °C). Variation of the temperature revealed that precursor was most effectively pyrolyzed at 800 °C for 2 h under Ar. Subsequent treatment with aqueous HCl solution overnight selectively removed inactive, agglomerated and unprotected iron particles generated during the pyrolysis process.

Structural characterization of the FeO_x@NGr−C system was carried out using various methods as shown in Figure 3. Obviously, larger iron nanoparticles were removed after selective leaching with HCl solution and only small nanoparticles (20−30 nm) remained (Figure 3a and Figure S1). As expected, high-resolution transmission electron microscopy (HRTEM) image revealed that all present nanoparticles were protected by graphene shells (Figure 3b and Figure S2). More specifically, 3−12 layers are observed which correspond to a thickness of 1.2−3.5 nm. Interestingly, some carbon nanotubes were observed on the surface as well. Most likely, the latter are left behind after removing the larger iron particles which cannot be protected well by the graphene shells (Figure S3). The iron/graphene core−shell structure was further proved by HAADF images. It is worth noting that the core−shell structure remained intact after using the catalyst several times, demonstrating the stability of the FeO_x@NGr−C architecture (Figure S4). From the XRD analysis, the broad reflections at about 25° and 44° are from the C-support (Figure S5). In addition, a sample pyrolyzed at higher temperature (1000 °C) showed sharper reflections caused by the crystalline phase Fe_3C and a small amount of FeN. XPS analysis revealed that the content of carbon grew with increasing pyrolysis temperature, whereas the content of N and Fe decreased due to the high temperature (Table S2). The content of the Fe dropped from 0.36% to 0.17% as the pyrolysis temperature increased from 600 to 800 °C, suggesting that the higher the pyrolysis temperature, the faster the agglomeration. However, increasing the temperature to 1000 °C left the content of iron almost unchanged. The peaks in the N 1s spectrum at 398.9 and 400.9 eV are assigned to pyrrolic N and graphitic N on the basis of the respective binding energies (Figure 3d). It is reported that the graphitic N plays a crucial role in the oxygen reduction,[10d] which might explain the high activity of the FeO_x@NGr−C catalyst. In addition, Fe^{2+} and Fe^{3+} were detected according to the corresponding binding energies at 710.2, 716.0, 722.1, and 726.1 eV after pyrolysis at 800 °C.

To examine the activity of the prepared catalysts for selective oxidative dehydrogenation of heterocycles, we initially tested different FeO_x@NGr−C materials with 1,2,3,4-tetrahydroquinoline as the model substrate. As shown in Table 1, FeO_x@NGr catalysts with or without aqueous HCl treatment gave similar product yields (entries 1 and 2). However, the pyrolyzed catalyst, which was washed subsequently with aqueous HCl, achieved higher TONs (267 and 106 mol/mol Fe, respectively). Compared to the nonwashed catalyst, no byproducts, such as quinolinone, were detected by GC and GC−MS analysis and full selectivity for the desired product was obtained. The better selectivity of the HCl-treated catalyst is attributed to the specific structure of FeO_x@NGr−C material, in which all the catalytically active iron species are confined with the graphene capsule. Apparently, this specific structure inhibits the interaction of the CH_2 group of 1,2,3,4-tetrahydroquinoline with the active site of the catalyst, so the

DOI: 10.1021/jacs.5b05674
J. Am. Chem. Soc. 2015, 137, 10652−10658

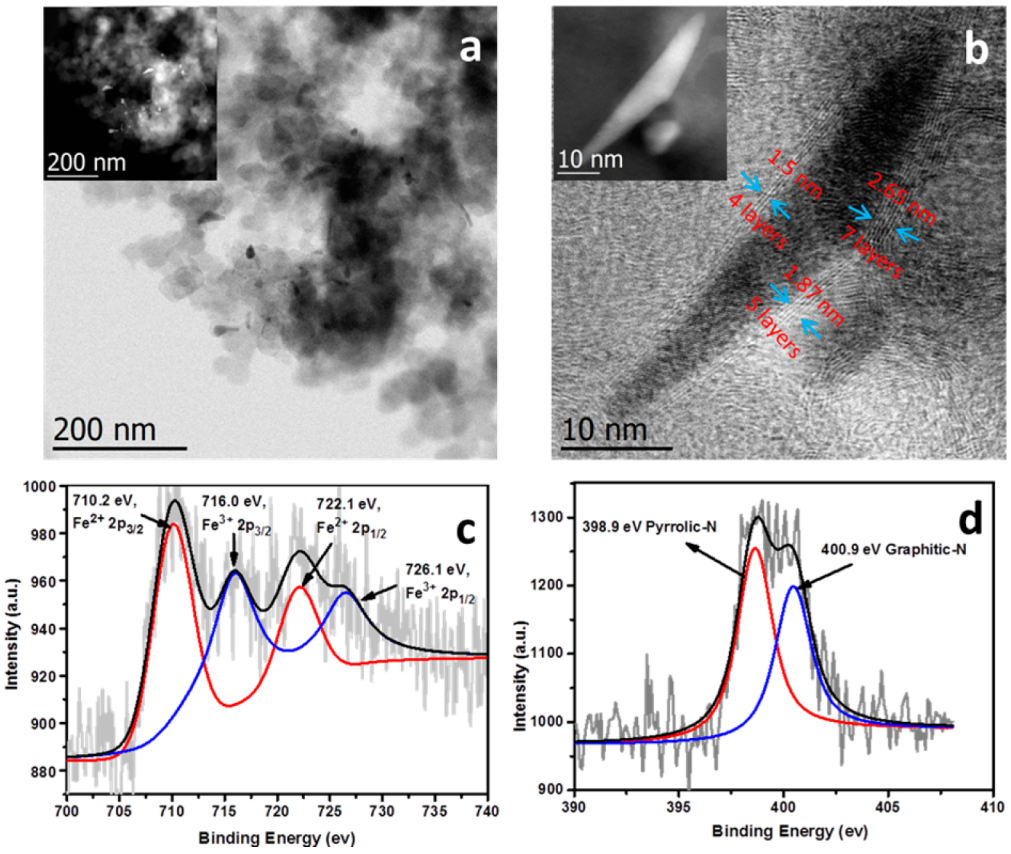

Figure 3. HRTEM images (a and b) of the FeO_x@NGr−C (inset of a and b: HAADF images), Fe 2p XPS spectrum (c), and N 1s XPS spectrum (d) of FeO_x@NGr−C.

formation of quinolinone is avoided. In contrast, without HCl washing, larger iron oxide nanoparticles are present at the surface, which show unspecific reactivity. As a control reaction, the carbon-supported iron oxide, i.e., FeO_x/C, was prepared in the absence of **L1** and lower activity was observed in the dehydrogenation reaction of 1,2,3,4-tetrahydroquinoline (entry 3). Pyrolysis of bare carbon and **L1** exhibited poor activities in the oxidation of 1,2,3,4-tetrahydroquinoline, too (entries 4 and 5). Notably, using SiO_2 and CeO_2 as supports gave also active materials, albeit the reactivity is somewhat lower (yields of quinoline: 23% and 21%, respectively; entries 6 and 7).

Next, different solvents were tested in the model reaction. In general, nonpolar solvents gave higher yields and the best yield (74%) was obtained when using heptane as solvent (entries 8−12). When the reaction temperature decreased to 80 °C, high selectivity but lower activity were obtained (entry 13). On the other hand, the catalytic activity is improved (85% yield) by increasing the air pressure to 15 bar (entry 14). We also tested the catalytic activity of $FeCl_2$ and $FeCl_3$ as catalyst precursors in the presence of the N-doped carbon, which are likely to be formed during the leaching procedure and absorbed on the catalyst. In this context, the activities were very low (Table 1, entries 15 and 16). When the air pressure increased to 20 bar, the yield was decreased to 77% because quinolinone was detected (entry 17). When the reaction was carried out with diluted O_2, 83% yield was obtained (entry 18). Furthermore, the pyrolysis temperature was varied in the range between 600 and 1000 °C, and the corresponding results suggest that 800 °C is the optimized temperature (Table S1, entries 1 and 2). Interestingly, when **L2**−**L5** were chosen as ligands instead of **L1**, 6−49% yield of quinoline was observed under the same reaction conditions (Table S1, entries 3−7).

In heterogeneous catalysis, it is still challenging to avoid the aggregation and leaching of the active metal during the reaction, which often results in deactivation of the catalysts. So the reusability of our NGr-modified catalyst (FeO_x@NGr−C) in the dehydrogenation of 1,2,3,4-tetrahydroquinoline was tested. For this purpose, the active material was separated from the reaction mixture via simple centrifugation, and reused directly for 5 times. To our delight, no obvious deactivation was observed. The yield of the desired product amounted to 79% at the fifth cycle and the total TONs were 2317 (Figure 4). Additionally, no further reaction was observed, when the catalyst was filtered off and another portion of substrate was added. Hence, the catalytically active species should not be derived from the leached metals.

Since FeO_x@NGr−C displayed the best activity for the production of quinoline, it was deployed in the scope study under the optimized conditions. As shown in Table 2, substituents at the 3 or 4 positions are well tolerated, and 3-methylquinoline (**2b**) and 4-methylquinoline (**2c**) were produced with 77% and 85% yields, respectively (entries 2 and 3). However, more sterically hindered functional groups, such as 2-methyl, 2-phenyl, and 2-tetrahydroquinoline derivatives (**1d**−**1f**), were converted to the corresponding quinolines in 51%−67% yields (entries 4−6). As expected, higher yields were obtained using FeO_x@NGr−C−NL as catalyst. Substituted quinolines at the 6 position on the aromatic ring were obtained in high yields too. Electron-donating groups such as

DOI: 10.1021/jacs.5b05674
J. Am. Chem. Soc. 2015, 137, 10652−10658

Table 1. Model Reaction: Study of Reaction Conditions[a]

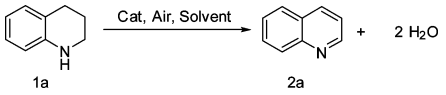

entry	catalyst	solvent	con (%)	Y (%)[b]	TON
1	FeO_x@NGr−C-NL	CH_3CN	63	46	106
2	FeO_x@NGr−C	CH_3CN	48	48	267
3	FeO_x/C	CH_3CN	17	15	5
4	C	CH_3CN	13	10	--
5	L1/C	CH_3CN	6	4	--
6	Fe/L1/SiO_2	CH_3CN	24	23	7
7	Fe/L1/CeO_2	CH_3CN	21	21	6
8	FeO_x@NGr−C	H_2O	18	18	100
9	FeO_x@NGr−C	CH_3OH	38	37	205
10	FeO_x@NGr−C	Toluene	40	39	217
11	FeO_x@NGr−C	Xylene	36	36	200
12	FeO_x@NGr−C	Heptane	75	74	411
13	FeO_x@NGr−C	Heptane	44	43[c,d]	239
14	FeO_x@NGr−C	Heptane	85	85[c]	472
15	$FeCl_2$ + L1/C	Heptane	0	10[c]	5
16	$FeCl_3$ + L1/C	Heptane	0	7[c]	4
17	FeO_x@NGr−C	Heptane	100	77[e]	427
18	FeO_x@NGr−C	Heptane	100	83[f]	461

[a]Reaction conditions: 0.5 mmol 1,2,3,4-tetrahydroquinoline, 30 mg catalyst (0.18 mol % Fe, 10 bar air, 2 mL solvent, 100 °C, 12 h, NL = No Leaching. For entries 15 and 16, 1.0 mol % Fe and 30 mg **L1**/C were used. [b]The yields were obtained by GC using dodecane as internal standard. [c]15 bar air. [d]80 °C. [e]20 bar air. [f]8% O_2 in N_2, 40 bar. Warning: the upper flammable limit for heptane is 6.7%, the reaction was operated far away from igniting sources.

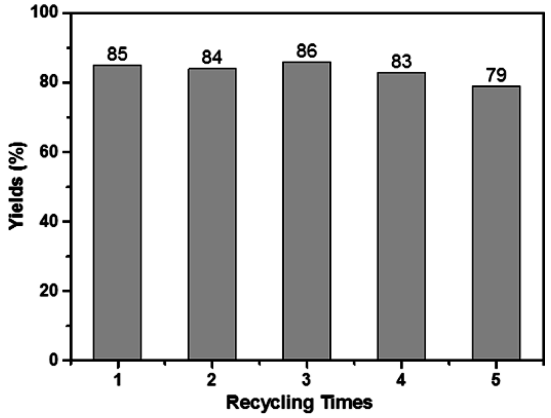

Figure 4. Oxidation of 1,2,3,4-tetrahydroquinoline: recycling of the FeO_x@NGr−C catalyst. Reaction conditions: 0.5 mmol substrate, 30 mg catalyst (0.18 mol % Fe), 2 mL heptane, 15 bar air, 100 °C, 12 h. Yields were determined by GC.

methoxy, ester, and methyl (**1g**−**1i**) had no significant influence on the activity of this catalytic system (entries 7−9).

Similarly, substrates bearing electron-withdrawing functional groups were also active. Thus, 6-bromoquinoline (**2j**) and 6-chloroquinoline (**2k**) were obtained in 85% and 88% yields (entries 10 and 11). Gratifyingly, products containing more-electron-withdrawing groups such as quinolone-6-carboxylic acid (**2l**), 6-nitroquinoline (**2m**) and 6-trifluoromethyl-quinoline (**2n**) were isolated in yields up to 89% (entries 12−14). Different groups at 8 position of the aromatic ring (**1o**−**1q**) did not exert a marked influence on the outcome of the reaction as all of the starting materials gave good to excellent yields (entries 15−17). In addition, 2,6-, 2,7-, and 2,8-disubstituted substrates with different functional groups (**1r**−**1u**) were also tested and the desired products were generated in 54−85% yield (entries 18−21). Remarkably, 4,7-dichloro-1,2,3,4-tetrahydroquinoline (**1v**) was also successfully converted to the corresponding quinoline with 69% yield (entry 22). Boron-containing compounds are important motifs in life sciences, so **1w** was tested as starting material (entry 23). Interestingly, 6-(4,4,5,5-tetramethyl-1,3,2-dioxaborolan-2-yl)quinoline (**2w**) was successfully synthesized in 70% yield.

Meanwhile, as shown in Table 3, the FeO_x@NGr−C catalyst displayed good activity in the oxidative formation of 1,2,3,4-tetrahydro-1,10-phenanthroline (**4b**) from 1,2,3,4,7,8,9,10-octahydro-1,10-phenanthroline (entry 2). Apart from quinoline derivatives, quinoxaline (**4a**), acridine (**4c**), quinoxaline (**4d**), isoquinoline (**4e**) and indole (**4f**) were also generated in 85%−93% yield under optimized reaction conditions (entries 1, 3−6).

The high reactivity of the tetrahydroquinoline derivatives encouraged us to test the FeO_x@NGr−C catalyst for the dehydrogenation of selected interesting bioactive compounds. As an example, the intermediate in the synthesis of the nM5-lipoxygenase inhibitor, **6a**, was obtained in 69% isolated yield. Moreover, both dehydrogenation and oxidation of the benzylic group occurred when **5b**[13a] was employed as substrate and **6b** is obtained in 65% yield. This heterocycle is an important motif in numerous biologically active compounds (Scheme 1 and Scheme S1).

Furthermore, the selective oxidation of amines was also examined using the FeO_x@NGr−C catalyst. As shown in Table 4, the dehydrogenations of *N*-benzylaniline and *N*-butylaniline occurred smoothly and the corresponding imines are obtained in 75% and 81% yield, respectively. In addition, dibenzylamine was converted to the desired product in 83% yields.

To get insights into the mechanism of the FeO_x@NGr−C-catalyzed dehydrogenation of heterocycles, the oxidation of 1,2,3,4-tetrahydroquinoline in the presence of butylated hydroxytoluene (BHT) was investigated. Notably, in the presence of this radical scavenger, no quinoline was formed, suggesting that the reaction progressed by radical species, e.g., the superoxide radical anion ($\cdot O_2^-$). It is well-known that BHT suppresses the formation of $\cdot O_2^-$.[10c,d] We assume that under catalytic conditions the nitrogen-doped graphene-like carbon materials are able to reduce absorbed O_2 to $\cdot O_2^-$. Despite several trials, the generation of H_2O_2 was never observed; hence, we assume that H_2O_2 is quickly consumed on forming quinoline and water (Scheme 2). Furthermore, EPR analysis revealed the formation of radical **A** (Figure S6), which is in agreement with the proposed catalytic pathway. In addition, the used FeO_x@NGr−C was analyzed by XPS. Interestingly, the content of Fe^{3+} is decreased and binding energies for Fe^{2+} are moved to 710.8 and 723.9 eV, which suggests that the synergism between Fe^{2+} and Fe^{3+} species influences the activity during the reaction (Figure S7).

Indeed, the oxidation of **1a** succeeded even at lower temperature (80 °C) with desired product formed in 78% yield if H_2O_2 is used as the oxidant instead of air. As shown in Table 3, the catalytic dehydrogenation of 1,2,3,4-tetrahydroquinoxaline occurred and the product quinoxaline (**4d**) was generated in quantitative yield suggesting that the oxidation sequence commences with the formation of the corresponding imine (C═N). The final product is obtained by another

DOI: 10.1021/jacs.5b05674
J. Am. Chem. Soc. 2015, 137, 10652−10658

Table 2. Oxidation of Tetrahydroquinolines Catalyzed by FeO_x@NGr−C[a]

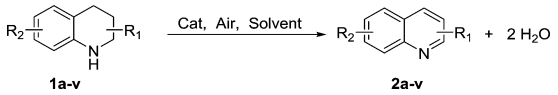

1a-v 2a-v

Entry	Substrates	Products	Y (%)[b]
1	 (1a)	 (2a)	83
2	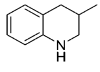 (1b)	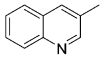 (2b)	77
3	 (1c)	 (2c)	85
4	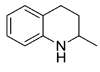 (1d)	 (2d)	67 (74)
5	 (1e)	 (2e)	63 (77)
6	 (1f)	 (2f)	51 (71)
7	 (1g)	 (2g)	81
8	 (1h)	 (2h)	89
9	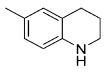 (1i)	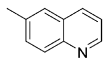 (2i)	84
10	 (1j)	 (2j)	85
11	 (1k)	 (2k)	88
12	 (1l)	 (2l)	85[c]
13	 (1m)	 (2m)	89[c]
14	 (1n)	 (2n)	84
15	 (1o)	 (2o)	88
16	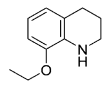 (1p)	 (2p)	69
17	 (1q)	 (2q)	93[c]
18	 (1r)	 (2r)	88
19	 (1s)	 (2s)	84
20	 (1t)	(2t)	75
21	(1u)	(2u)	54
22	(1v)	(2v)	62
23	(1w)	(2w)	70

[a]Reaction conditions: 0.5 mmol substrate, 30 mg catalyst (0.18 mol % Fe), 2 mL heptane, 15 bar air, 100 °C, 12 h. The yields in parentheses were obtained using FeO_x@NGr−C-NL. [b]Isolated yields. [c]CH_3CN as solvent, 24 h.

dehydrogenation reaction, which probably takes place after tautomerization as investigated by Jones and co-workers.[11e]

In agreement with this proposal, no dehydrogenation product was detected when using 2,2,4-trimethyl-1,2,3,4-tetrahydroquinoline (**9a**) as substrate (Scheme 3). Furthermore, the dehydrogenation of 1-(indolin-1-yl)ethan-1-one (**9b**) was also not observed, which suggests that the direct formation of a C=C linkage is difficult. This result also demonstrates that the presence of the N−H motif in the cycloalkane is critical for the dehydrogenation, which might be favorable for the adsorption of the starting material onto the catalyst surface.

CONCLUSION

In summary, we demonstrated for the first time that nanostructured iron oxides surrounded by nitrogen-doped-graphene shells immobilized on carbon support (labeled FeO_x@NGr−C) constitute an active catalyst for the dehydrogenation of *N*-heterocycles. The catalytic material is easily obtained in a practical and scalable two-step method via

DOI: 10.1021/jacs.5b05674
J. Am. Chem. Soc. 2015, 137, 10652−10658

Table 3. Oxidation of *N*-Heterocycles Catalyzed by FeO_x@NGr−C[a]

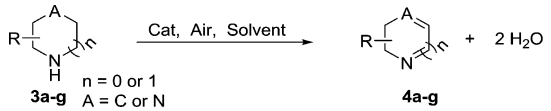

Entry	Substrates	Products	Y (%)[b]
1	(3a)	(4a)	83
2	(3b)	(4b)	78
3	(3c)	(4c)	87
4	(3d)	(4d)	93
5	(3e)	(4e)	79
6	(3f)	(4f)	92

[a]Reaction conditions: 0.5 mmol substrate, 30 mg catalyst (0.18 mol % Fe), 2 mL heptane, 15 bar air, 100 °C, 12 h. [b]Isolated yields.

Scheme 1. Synthesis of Pharmaceutical Relevant Intermediates 6a and 6b

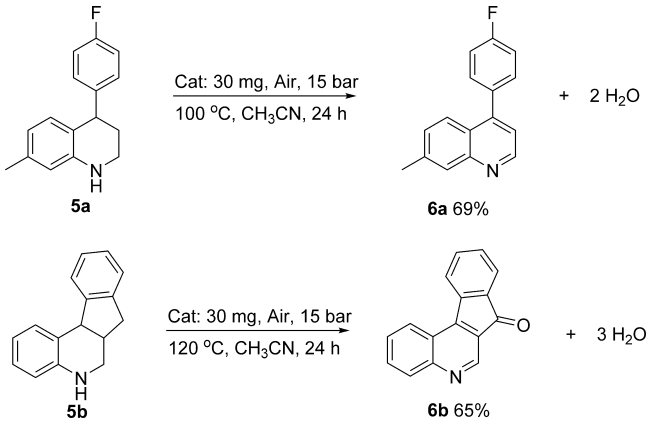

Table 4. Oxidation of Amines Catalyzed by FeO_x@NGr−C[a]

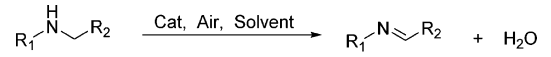

Entry	Substrate	Product	Y (%)[b]
1	(7a)	(8a)	75
2	(7b)	(8b)	81
3	(7c)	(8c)	83

[a]Reaction conditions: 0.5 mmol substrate, 30 mg catalyst (0.18 mol % Fe), 2 mL heptane, 15 bar air, 100 °C, 12 h. [b]GC yields.

Scheme 2. Proposed Catalytic Pathway for the Dehydrogenation of *N*-Heterocycles

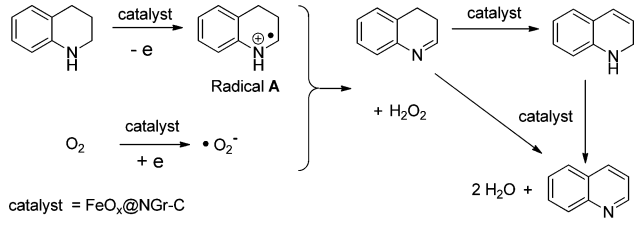

Scheme 3. Control Experiments

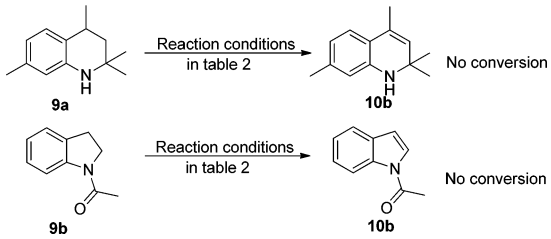

pyrolysis of simple iron acetate and phenanthroline and subsequent selective leaching. The optimized material allows for green dehydrogenations of several *N*-heterocycles. The utility of the methodology is also highlighted by the synthesis of pharmaceutically relevant quinolines.

■ ASSOCIATED CONTENT

Supporting Information

The Supporting Information is available free of charge on the ACS Publications website at DOI: 10.1021/jacs.5b05674.

Extended data about optimization of reaction conditions; preparation, characterization and recovery of FeO_x@NGr−C; mechanism investigations and synthesis and spectroscopic data of products (PDF)

■ AUTHOR INFORMATION

Corresponding Author

*matthias.beller@catalysis.de

Notes

The authors declare no competing financial interest.

■ ACKNOWLEDGMENTS

This work was supported by the state of Mecklenburg Vorpommern and F. Hoffmann-La Roche. We thank Dr. Carsten Kreyenschulte, Dr. Jabor Rabeah and Dr. Jörg Radnik for technical assistance.

■ REFERENCES

(1) (a) Sun, C. L.; Li, B. J.; Shi, Z. J. *Chem. Rev.* **2011**, *111*, 1293. (b) Riener, K.; Haslinger, S.; Raba, A.; Hogerl, M. P.; Cokoja, M.; Herrmann, W. A.; Kuhn, F. E. *Chem. Rev.* **2014**, *114*, 5215. (c) Liu, J.; Chakraborty, S.; Hosseinzadeh, P.; Yu, Y.; Tian, S. L.; Petrik, I.; Bhagi, A.; Lu, Y. *Chem. Rev.* **2014**, *114*, 4366. (d) Gopalaiah, K. *Chem. Rev.* **2013**, *113*, 3248. (e) Bolm, C.; Legros, J.; Le Paih, J.; Zani, L. *Chem. Rev.* **2004**, *104*, 6217.

(2) (a) Tondreau, A. M.; Atienza, C. C. H.; Weller, K. J.; Nye, S. A.; Lewis, K. M.; Delis, J. G. P.; Chirik, P. J. *Science* **2012**, *335*, 567. (b) Hoyt, J. M.; Sylvester, K. T.; Sernproni, S. P.; Chirik, P. J. *J. Am. Chem. Soc.* **2013**, *135*, 4862. (c) Gulak, S.; Jacobi von Wangelin, A. *Angew. Chem., Int. Ed.* **2012**, *51*, 1357. (d) Gartner, D.; Welther, A.; Rad, B. R.; Wolf, R.; Jacobi von Wangelin, A. *Angew. Chem., Int. Ed.*

DOI: 10.1021/jacs.5b05674
J. Am. Chem. Soc. 2015, 137, 10652−10658

2014, *53*, 3722. (e) Fillol, J. L.; Codola, Z.; Garcia-Bosch, I.; Gomez, L.; Pla, J. J.; Costas, M. *Nat. Chem.* **2011**, *3*, 807. (f) Darmon, J. M.; Stieber, S. C. E.; Sylvester, K. T.; Fernandez, I.; Lobkovsky, E.; Semproni, S. P.; Bill, E.; Wieghardt, K.; DeBeer, S.; Chirik, P. J. *J. Am. Chem. Soc.* **2012**, *134*, 17125. (g) Cusso, O.; Garcia-Bosch, I.; Ribas, X.; Lloret-Fillol, J.; Costas, M. *J. Am. Chem. Soc.* **2013**, *135*, 14871. (h) Costas, M.; Mehn, M. P.; Jensen, M. P.; Que, L. *Chem. Rev.* **2004**, *104*, 939. (i) Company, A.; Sabenya, G.; Gonzalez-Bejar, M.; Gomez, L.; Clemancey, M.; Blondin, G.; Jasniewski, A. J.; Puri, M.; Browne, W. R.; Latour, J. M.; Que, L.; Costas, M.; Perez-Prieto, J.; Lloret-Fillol, J. *J. Am. Chem. Soc.* **2014**, *136*, 4624.

(3) (a) Takahashi, K.; Wang, Y. M.; Chiba, S.; Nakagawa, Y.; Isobe, S.; Ohnuki, S. *Sci. Rep.* **2014**, *4*, 4598. (b) Sonnenberg, J. F.; Coombs, N.; Dube, P. A.; Morris, R. H. *J. Am. Chem. Soc.* **2012**, *134*, 5893. (c) Moussa, S. O.; Panchakarla, L. S.; Ho, M. Q.; El-Shall, M. S. *ACS Catal.* **2014**, *4*, 535. (d) Li, L.; Lv, J. G.; Shen, Y.; Guo, X. F.; Peng, L. M.; Xie, Z. K.; Ding, W. P. *ACS Catal.* **2014**, *4*, 2746. (e) Hu, Y.; Jensen, J. O.; Zhang, W.; Cleemann, L. N.; Xing, W.; Bjerrum, N. J.; Li, Q. F. *Angew. Chem., Int. Ed.* **2014**, *53*, 3675. (f) Torres Galvis, H. M.; Bitter, J. H.; Khare, C. B.; Ruitenbeek, M.; Dugulan, A. I.; de Jong, K. P. *Science* **2012**, *335*, 835. (g) Dey, R.; Mukherjee, N.; Ahammed, S.; Ranu, B. C. *Chem. Commun.* **2012**, *48*, 7982. (h) Chen, G. X.; Zhao, Y.; Fu, G.; Duchesne, P. N.; Gu, L.; Zheng, Y. P.; Weng, X. F.; Chen, M. S.; Zhang, P.; Pao, C. W.; Lee, J. F.; Zheng, N. F. *Science* **2014**, *344*, 495.

(4) (a) Mahmoudi, M.; Hofmann, H.; Rothen-Rutishauser, B.; Petri-Fink, A. *Chem. Rev.* **2012**, *112*, 2323. (b) Tian, J.; Morozan, A.; Sougrati, M. T.; Lefevre, M.; Chenitz, R.; Dodelet, J. P.; Jones, D.; Jaouen, F. *Angew. Chem., Int. Ed.* **2013**, *52*, 6867. (c) Kramm, U. I.; Lefevre, M.; Larouche, N.; Schmeisser, D.; Dodelet, J. P. *J. Am. Chem. Soc.* **2014**, *136*, 978. (d) Lin, L.; Zhu, Q.; Xu, A. W. *J. Am. Chem. Soc.* **2014**, *136*, 11027. (e) Riener, K.; Haslinger, S.; Raba, A.; Hogerl, M. P.; Cokoja, M.; Herrmann, W. A.; Kuhn, F. E. *Chem. Rev.* **2014**, *114*, 5215.

(5) (a) Zhang, S.; Hao, Y. Z.; Su, D.; Doan-Nguyen, V. V. T.; Wu, Y. T.; Li, J.; Sun, S. H.; Murray, C. B. *J. Am. Chem. Soc.* **2014**, *136*, 15921. (b) Tian, Q. W.; Hu, J. Q.; Zhu, Y. H.; Zou, R. J.; Chen, Z. G.; Yang, S. P.; Li, R. W.; Su, Q. Q.; Han, Y.; Liu, X. G. *J. Am. Chem. Soc.* **2013**, *135*, 8571. (c) Miyajima, D.; Araoka, F.; Takezoe, H.; Kim, J.; Kato, K.; Takata, M.; Aida, T. *Science* **2012**, *336*, 209. (d) Zhang, J. T.; Tang, Y.; Lee, K.; Min, O. Y. *Science* **2010**, *327*, 1634. (e) Mazumder, V.; Chi, M. F.; More, K. L.; Sun, S. H. *J. Am. Chem. Soc.* **2010**, *132*, 7848. (f) Chen, H. M.; Deng, C. H.; Zhang, X. M. *Angew. Chem., Int. Ed.* **2010**, *49*, 607. (g) Li, L.; Feng, Y. J.; Li, Y. S.; Zhao, W. R.; Shi, J. L. *Angew. Chem., Int. Ed.* **2009**, *48*, 5888. (h) Xu, Z. C.; Hou, Y. L.; Sun, S. H. *J. Am. Chem. Soc.* **2007**, *129*, 8698. (i) Lauhon, L. J.; Gudiksen, M. S.; Wang, C. L.; Lieber, C. M. *Nature* **2002**, *420*, 57.

(6) (a) Li, G. L.; Mohwald, H.; Shchukin, D. G. *Chem. Soc. Rev.* **2013**, *42*, 3628. (b) Ghosh Chaudhuri, R.; Paria, S. *Chem. Rev.* **2012**, *112*, 2373.

(7) (a) Laurent, S.; Forge, D.; Port, M.; Roch, A.; Robic, C.; Elst, L. V.; Muller, R. N. *Chem. Rev.* **2010**, *110*, 2574. (b) Shui, J. L.; Karan, N. K.; Balasubramanian, M.; Li, S. Y.; Liu, D. J. *J. Am. Chem. Soc.* **2012**, *134*, 16654.

(8) (a) Bashyam, R.; Zelenay, P. *Nature* **2006**, *443*, 63. (b) Chung, H. T.; Won, J. H.; Zelenay, P. *Nat. Commun.* **2013**, *4*, 1922. (c) Lefevre, M.; Proietti, E.; Jaouen, F.; Dodelet, J. P. *Science* **2009**, *324*, 71. (d) Wu, G.; More, K. L.; Johnston, C. M.; Zelenay, P. *Science* **2011**, *332*, 443.

(9) (a) Jagadeesh, R. V.; Surkus, A. E.; Junge, H.; Pohl, M. M.; Radnik, J.; Rabeah, J.; Huan, H. M.; Schunemann, V.; Bruckner, A.; Beller, M. *Science* **2013**, *342*, 1073. (b) Jagadeesh, R. V.; Junge, H.; Beller, M. *Nat. Commun.* **2014**, *5*, 4123. (c) Stemmler, T.; Surkus, A. E.; Pohl, M. M.; Junge, K.; Beller, M. *ChemSusChem* **2014**, *7*, 3012.

(10) (a) Su, F. Z.; Mathew, S. C.; Mohlmann, L.; Antonietti, M.; Wang, X. C.; Blechert, S. *Angew. Chem., Int. Ed.* **2011**, *50*, 657. (b) Li, X. H.; Chen, J. S.; Wang, X. C.; Sun, J. H.; Antonietti, M. *J. Am. Chem. Soc.* **2011**, *133*, 8074. (c) Su, F. Z.; Mathew, S. C.; Lipner, G.; Fu, X. Z.; Antonietti, M.; Blechert, S.; Wang, X. C. *J. Am. Chem. Soc.* **2010**, *132*, 16299. (d) Strelko, V. V.; Kartel, N. T.; Dukhno, I. N.; Kuts, V. S.; Clarkson, R. B.; Odintsov, B. M. *Surf. Sci.* **2004**, *548*, 281.

(11) (a) Yamaguchi, R.; Ikeda, C.; Takahashi, Y.; Fujita, K. *J. Am. Chem. Soc.* **2009**, *131*, 8410. (b) Tseng, K. N. T.; Rizzi, A. M.; Szymczak, N. K. *J. Am. Chem. Soc.* **2013**, *135*, 16352. (c) Fujita, K.; Tanaka, Y.; Kobayashi, M.; Yamaguchi, R. *J. Am. Chem. Soc.* **2014**, *136*, 4829. (d) Adkins, h.; Hager, g. *J. Am. Chem. Soc.* **1949**, *71*, 2962. (e) Chakraborty, S.; Brennessel, W. W.; Jones, W. D. *J. Am. Chem. Soc.* **2014**, *136*, 8564. (f) Wang, Z. H.; Tonks, I.; Belli, J.; Jensen, C. M. *J. Organomet. Chem.* **2009**, *694*, 2854. (g) Wang, Z. H.; Belli, J.; Jensen, C. M. *Faraday Discuss.* **2011**, *151*, 297. (h) Crabtree, R. H. *Energy Environ. Sci.* **2008**, *1*, 134. (i) Dobereiner, G. E.; Crabtree, R. H. *Chem. Rev.* **2010**, *110*, 681. (j) Yao, W. B.; Zhang, Y. X.; Jia, X. Q.; Huang, Z. *Angew. Chem., Int. Ed.* **2014**, *53*, 1390. (k) Wu, J. J.; Talwar, D.; Johnston, S.; Yan, M.; Xiao, J. L. *Angew. Chem., Int. Ed.* **2013**, *52*, 6983. (l) Talwar, D.; Gonzalez-de-Castro, A.; Li, H. Y.; Xiao, J. L. *Angew. Chem., Int. Ed.* **2015**, *54*, 5223. (m) Muthaiah, S.; Hong, S. H. *Adv. Synth. Catal.* **2012**, *354*, 3045.

(12) (a) Hara, T.; Mori, K.; Mizugaki, T.; Ebitani, K.; Kaneda, K. *Tetrahedron Lett.* **2003**, *44*, 6207. (b) Damodara, D.; Arundhathi, R.; Likhar, P. R. *Adv. Synth. Catal.* **2014**, *356*, 189. (c) Amende, M.; Gleichweit, C.; Werner, K.; Schernich, S.; Zhao, W.; Lorenz, M. P. A.; Hofert, O.; Papp, C.; Koch, M.; Wasserscheid, P.; Laurin, M.; Steinruck, H. P.; Libuda, J. *ACS Catal.* **2014**, *4*, 657.

(13) (a) Wendlandt, A. E.; Stahl, S. S. *J. Am. Chem. Soc.* **2014**, *136*, 11910. (b) Iosub, A. V.; Stahl, S. S. *J. Am. Chem. Soc.* **2015**, *137*, 3454.

(14) (a) Jawale, D. V.; Gravel, E.; Shah, N.; Dauvois, V.; Li, H. Y.; Namboothiri, I. N. N.; Doris, E. *Chem. - Eur. J.* **2015**, *21*, 7039. (b) Furukawa, S.; Suga, A.; Komatsu, T. *Chem. Commun.* **2014**, *50*, 3277. (c) Ge, D. H.; Hu, L.; Wang, J. Q.; Li, X. M.; Qi, F. Q.; Lu, J. M.; Cao, X. Q.; Gu, H. W. *ChemCatChem* **2013**, *5*, 2183. (d) Yamaguchi, K.; Kim, J. W.; He, J. L.; Mizuno, N. *J. Catal.* **2009**, *268*, 343. (e) So, M. H.; Liu, Y. G.; Ho, C. M.; Che, C. M. *Chem. - Asian J.* **2009**, *4*, 1551. (f) Li, F.; Chen, J.; Zhang, Q.; Wang, Y. *Green Chem.* **2008**, *10*, 553. (g) Kamata, K.; Kasai, J.; Yamaguchi, K.; Mizuno, N. *Org. Lett.* **2004**, *6*, 3577. (h) Yamaguchi, K.; Mizuno, N. *Angew. Chem., Int. Ed.* **2003**, *42*, 1480. (i) Yamaguchi, K.; Mizuno, N. *Chem. - Eur. J.* **2003**, *9*, 4353. (j) Yuan, H.; Yoo, W. J.; Miyamura, H.; Kobayashi, S. *J. Am. Chem. Soc.* **2012**, *134*, 13970. (k) Choi, H.; Doyle, M. P. *Chem. Commun.* **2007**, 745.

(15) (a) Jagadeesh, R. V.; Junge, H.; Pohl, M. M.; Radnik, J.; Bruckner, A.; Beller, M. *J. Am. Chem. Soc.* **2013**, *135*, 10776. (b) Westerhaus, F. A.; Jagadeesh, R. V.; Wienhofer, G.; Pohl, M. M.; Radnik, J.; Surkus, A. E.; Rabeah, J.; Junge, K.; Junge, H.; Nielsen, M.; Bruckner, A.; Beller, M. *Nat. Chem.* **2013**, *5*, 537. (c) Stemmler, T.; Westerhaus, F. A.; Surkus, A. E.; Pohl, M. M.; Junge, K.; Beller, M. *Green Chem.* **2014**, *16*, 4535. (d) Banerjee, D.; Jagadeesh, R. V.; Junge, K.; Pohl, M. M.; Radnik, J.; Bruckner, A.; Beller, M. *Angew. Chem., Int. Ed.* **2014**, *53*, 4359.

DOI: 10.1021/jacs.5b05674
J. Am. Chem. Soc. 2015, 137, 10652−10658